



Published in final edited form as:

Nat Chem Biol. 2009 January ; 5(1): 37–44. doi:10.1038/nchembio.129.

## Selective blockade of 2-arachidonoylglycerol hydrolysis produces cannabinoid behavioral effects

Jonathan Z. Long<sup>1</sup>, Weiwei Li<sup>1</sup>, Lamont Booker<sup>2</sup>, James J. Burston<sup>3</sup>, Steven G. Kinsey<sup>3</sup>, Joel E. Schlosburg<sup>3</sup>, Franciso J. Pavón<sup>2</sup>, Antonia M. Serrano<sup>2</sup>, Dana E. Selley<sup>3</sup>, Loren H. Parsons<sup>2</sup>, Aron H. Lichtman<sup>3</sup>, and Benjamin F. Cravatt<sup>1,\*</sup>

<sup>1</sup>The Skaggs Institute for Chemical Biology and Department of Chemical Physiology, The Scripps Research Institute, 10550 N. Torrey Pines Rd. La Jolla, CA 92037

<sup>2</sup>Committee on the Neurobiology of Addiction, The Scripps Research Institute, 10550 N. Torrey Pines Rd. La Jolla, CA 92037

<sup>3</sup>Department of Pharmacology and Toxicology, Virginia Commonwealth University, 410 North 12<sup>th</sup> Street. Richmond, VA 23298

### Abstract

2-Arachidonoylglycerol (2-AG) and anandamide are endocannabinoids that activate cannabinoid receptors CB1 and CB2. Endocannabinoid signaling is terminated by enzymatic hydrolysis, a process that, for anandamide, is mediated by fatty acid amide hydrolase (FAAH) and, for 2-AG, is thought to involve monoacylglycerol lipase (MAGL). FAAH inhibitors produce a select subset of the behavioral effects observed with CB1 agonists, intimating a functional segregation of endocannabinoid signaling pathways *in vivo*. Testing this hypothesis, however, requires specific tools to independently block anandamide and 2-AG metabolism. Here, we report a potent and selective inhibitor of MAGL, JZL184, that, upon administration to mice, raises brain 2-AG by 8-fold without altering anandamide. JZL184-treated mice exhibited a broad array of CB1-dependent behavioral effects, including analgesia, hypothermia, and hypomotility. These data indicate that 2-AG endogenously modulates several behavioral processes classically associated with the pharmacology of cannabinoids and point to overlapping and unique functions for 2-AG and anandamide *in vivo*.

The cannabinoid receptors CB1 and CB2 are molecular targets for <sup>9</sup>-tetrahydrocannabinol (**1**), the psychoactive component of marijuana<sup>1</sup>. Two endogenous ligands, or “endocannabinoids,” have also been identified, the arachidonate-based lipids anandamide (*N*-arachidonoyl ethanolamine, AEA, **2**) and 2-arachidonoylglycerol (2-AG, **3**)<sup>2-4</sup>. The endocannabinoid system regulates a range of physiological processes, including appetite<sup>5</sup>, pain sensation<sup>6</sup>, inflammation<sup>7</sup>, and memory<sup>8,9</sup>, and is the current focus of considerable

Users may view, print, copy, and download text and data-mine the content in such documents, for the purposes of academic research, subject always to the full Conditions of use:[http://www.nature.com/authors/editorial\\_policies/license.html#terms](http://www.nature.com/authors/editorial_policies/license.html#terms)

\*To whom correspondence should be addressed: cravatt@scripps.edu.

**Author contributions.** J.Z.L., L.H.P., A.H.L., and B.F.C. designed the experiments. J.Z.L. and W.L. synthesized and characterized the inhibitors. L.B., F.J.P., A.M.S., and L.H.R. measured extracellular endocannabinoid levels. J.J.B., S.G.K., J.E.S., D.E.S., and A.H.L. performed behavioral studies. J.Z.L. and B.F.C. wrote the manuscript.

pharmaceutical interest to treat disorders such as obesity, chronic pain, anxiety, and depression<sup>10</sup>.

Endocannabinoid signaling is tightly controlled by enzymatic hydrolysis<sup>11</sup>. The principal AEA-hydrolyzing enzyme is fatty acid amide hydrolase (FAAH)<sup>12</sup>. Genetic<sup>13</sup> or pharmacological<sup>14,15</sup> disruption of FAAH causes significant elevations in AEA levels throughout the nervous system and periphery, resulting in multiple CB1- and/or CB2-dependent behavioral effects, including reduction in pain sensation, inflammation, anxiety, and depression<sup>16</sup>. Interestingly, several of the other well-known behavioral effects of direct CB1 agonists, such as hypothermia and movement disorders, are not observed in FAAH-disrupted animals<sup>14,17</sup>. These animals also possess wild-type levels of 2-AG, which suggests that additional CB1-regulated behavioral processes may be mediated by 2-AG *in vivo*. Uncoupling AEA and 2-AG-dependent signaling by selective pharmacological blockade of their respective degradative enzymes could directly address this hypothesis.

Several lines of evidence suggest that monoacylglycerol lipase (MAGL) is a primary enzyme responsible for hydrolyzing 2-AG in the nervous system. First, recombinant expression of MAGL reduces receptor-dependent 2-AG accumulation in cortical neurons<sup>18</sup>. Second, immunodepletion of MAGL decreases 2-AG hydrolysis activity in rat brain tissue by 50%<sup>19</sup>. Third, a comprehensive survey of serine hydrolases in the mouse brain has ascribed ~85% of total 2-AG hydrolysis activity in this tissue to MAGL<sup>20</sup>. Finally, promiscuous serine hydrolase inhibitors that block MAGL (along with several other enzymes, including FAAH) dramatically raises brain 2-AG levels and produce cannabinoid behavioral effects in mice<sup>21</sup>. However, none of these previous studies have specifically examined the role that MAGL plays in hydrolyzing 2-AG *in vivo*. Toward this goal, several MAGL inhibitors have been described<sup>6,22,23</sup>, but none show the level of potency and specificity required for general use as *in vivo* pharmacological tools. For instance, arguably the most well-characterized MAGL inhibitor URB602 (**4**) displays an IC<sub>50</sub> value of ~200 μM<sup>23</sup> and is therefore insufficiently potent for systemic administration *in vivo*. Moreover, this compound has recently been reported to exhibit similar potencies for both MAGL and FAAH<sup>24</sup>, raising concerns about its utility to discriminate between 2-AG and AEA degradative pathways. A second MAGL inhibitor *N*-arachidonyl maleamide (NAM<sup>22</sup>, **5**) exhibits some selectivity for MAGL over FAAH and other serine hydrolases<sup>20</sup> and has been shown to potentiate the pharmacological effects of 2-AG *in vivo*<sup>25</sup>. However, the maleamide group of NAM is a general thiol-reactive electrophile and will therefore likely cause this inhibitor to react with many other cysteine-containing proteins and small molecules (e.g., glutathione) *in vivo*. Finally, considering further that several enzymes in addition to MAGL have been shown to hydrolyze 2-AG *in vitro*<sup>20</sup>, questions remain regarding the specific contribution that MAGL makes to 2-AG signaling *in vivo* and whether blockade of this pathway will produce behavioral effects indicative of heightened endocannabinoid tone.

Here we report the development of a potent and selective MAGL inhibitor, JZL184 (**6**) (Fig. 1a), that displays exceptional activity *in vivo*. Key to the success of this pharmacological program was the implementation of activity-based proteomic methods to broadly evaluate and optimize the selectivity of inhibitors across the serine hydrolase superfamily. JZL184

produced a rapid and sustained blockade of brain 2-AG hydrolase activity in mice, resulting in 8-fold elevations in endogenous 2-AG levels that were maintained for at least 8 h. In contrast, AEA levels were unaffected by JZL184. JZL184-treated mice showed a remarkable array of CB1-dependent behavioral effects, including analgesia, hypomotility, and hypothermia, that suggest a broad role for 2-AG-mediated endocannabinoid signaling throughout the mammalian nervous system.

## RESULTS

### Development of the MAGL inhibitor JZL184

The pursuit of selective inhibitors for serine hydrolases has the potential to benefit from multiple features special to this enzyme class. First, serine hydrolases are susceptible to covalent inactivation by specific chemical groups that show little or no cross-reactivity with other enzyme classes. Principal among these reactive chemotypes is the carbamate, which has been identified as a privileged scaffold for the design of selective, irreversible inhibitors of serine hydrolases owing to its tempered electrophilicity and hydrolytic stability following covalent reaction (carbamylation) with the conserved serine nucleophile of these enzymes<sup>26,27</sup>. Second, the functional state of serine hydrolases can be collectively profiled in native biological systems using activity-based protein profiling (ABPP) methods<sup>28</sup>. ABPP of serine hydrolases uses reporter-tagged fluorophosphonates (FPs), which serve as general activity-based probes for this large and diverse enzyme class<sup>29</sup>. When performed in a competitive mode, ABPP can serve as a powerful screen to evaluate the potency and selectivity of small-molecule enzyme inhibitors directly in complex proteomes<sup>30,31</sup>.

In the course of performing competitive ABPP screens with a structurally diverse library of carbamates<sup>27</sup>, we identified the compound WWL98 (**7**) (Supplementary Fig. 1 online), which inhibited a specific subset of brain serine hydrolases that included FAAH, MAGL and, ABHD6 (Fig. 1b). We next focused on modifying WWL98 to improve potency and selectivity for MAGL. The incorporation of a piperazine spacer and a distal bisaryl motif, as represented in WWL152 (**8**) and WWL162 (**9**) (Fig. 1a), was found to preserve potency for MAGL and ABHD6, while greatly reducing activity for FAAH (Fig. 1b). Replacement of the piperazine with a piperidinyl methanol scaffold afforded JZL175 (**10**) (Fig. 1a), a compound that exhibited selectivity for MAGL over both FAAH and ABHD6 (Fig. 1b). Finally, an additional two-fold enhancement in selectivity was achieved by inclusion of bis(methylene-3,4-dioxyphenyl) groups on the piperidinyl methanol scaffold to provide JZL184 (**Fig. 1a and b**; also see Supplementary Fig. 1 online).

### JZL184 is a potent and selective MAGL inhibitor

Near-complete blockade of MAGL activity was observed by competitive ABPP following a 30 min preincubation of a mouse brain membrane proteome with as low as 50 nM JZL184 (Fig 2a). In contrast, inhibition of other enzymes (FAAH, ABHD6) was not observed until much higher concentrations of JZL184 (10  $\mu$ M). Substrate assays confirmed this degree of selectivity, as JZL184 displayed IC<sub>50</sub> values of 8 nM and 4  $\mu$ M for blockade of 2-AG and oleamide (**11**) (FAAH substrate) hydrolysis in brain membranes, respectively (Fig. 2b). Comparable inhibitory effects were observed with recombinant MAGL and FAAH when

expressed in COS7 cells (Fig. 2c). Interestingly, brain membranes maintained a residual ~15% 2-AG hydrolysis activity even at the highest concentrations of JZL184 tested, likely reflecting the contribution of other 2-AG hydrolases that are insensitive to JZL18420. JZL184 displayed time-dependent inhibition of MAGL (Supplementary Fig. 2 online), indicative of a covalent mechanism of inactivation. We therefore also evaluated the relative activity of JZL184 for MAGL and FAAH by measuring  $k_{\text{obs}} [\text{I}]^{-1}$  values, which confirmed > 300-fold selectivity for inhibition of MAGL (4400 and 13  $\text{M}^{-1} \text{s}^{-1}$ , respectively). Finally, we tested JZL184 for activity on other components of the endocannabinoid system and enzymes involved in arachidonate metabolism. JZL184 did not interact with CB1 or CB2 receptors and did not inhibit the 2-AG biosynthetic enzymes diacylglycerol lipase- $\alpha$  and  $\beta$  or the arachidonic acid-mobilizing enzyme cytosolic phospholipase A<sub>2</sub> group IVA (Supplementary Fig. 3 online). Collectively, these data indicate that JZL184 potently and selectively inactivates MAGL in the mouse brain proteome.

### JZL184 inhibits MAGL *in vivo* and elevates 2-AG levels

To assess the ability of JZL184 to block MAGL *in vivo*, male C57Bl/6 mice were administered JZL184 (4–40  $\text{mg kg}^{-1}$ , i.p.) and sacrificed after 4 h for analysis. At the lowest dose of JZL184 tested (4  $\text{mg kg}^{-1}$ ), competitive ABPP of brain membrane proteomes revealed 75% MAGL inactivation with minimal effects (< 20% inhibition) on other brain serine hydrolases, including FAAH (Fig. 3a). These data were also confirmed for MAGL and FAAH by substrate assays (Fig. 3b). Residual brain 2-AG hydrolysis activity could be further reduced from 25% to 15% of control values by increasing the dose of JZL184 from 4 to 16  $\text{mg kg}^{-1}$  (Fig. 3b), which correlated with a near-complete blockade of MAGL activity as determined by competitive ABPP (Fig. 3a). FAAH was also inhibited in a dose-dependent manner, but even at 16  $\text{mg kg}^{-1}$  of JZL184, a substantial fraction of FAAH activity (~35%) remained intact as determined by competitive ABPP (Fig. 3a) or substrate (Fig. 3b) assays.

Although our gel-based ABPP analysis already suggested high selectivity for MAGL *in vivo*, the limited resolution of this method precluded a complete assessment of the functional state of brain serine hydrolases in JZL184-treated animals. We therefore examined brain proteomes using an advanced liquid chromatography-mass spectrometry (LC-MS) platform, termed ABPP-MudPIT, that displays enhanced resolution and sensitivity compared to gel-based ABPP32. Briefly, brain membrane proteomes from mice treated with JZL184 or vehicle were subjected to competitive ABPP with the biotinylated FP probe, FP-biotin29 (**12**). FP-biotin-labeled proteins were then enriched with avidin, digested on-bead with trypsin, analyzed by multidimensional LC-MS, and identified using the SEQUEST search algorithm. ABPP-MudPIT confirmed that JZL184 (16  $\text{mg kg}^{-1}$ , 4 hr) produced a near-complete blockade of MAGL activity and partial inhibition of FAAH (Fig. 3c). Strikingly, none of the other ~40 brain serine hydrolases profiled by ABPP-MudPIT were significantly affected by JZL184 (Fig. 3c and Supplementary Table 1 online). These data demonstrate that, even when administered at a high dose (16  $\text{mg kg}^{-1}$ ) for an extended period of time (4 h), JZL184 maintains exceptional selectivity for MAGL in brain.

Having established the selectivity profile of JZL184 *in vivo*, we next measured brain levels of candidate endogenous substrates and products for MAGL and FAAH. Even at the lowest

dose of JZL184 tested ( $4 \text{ mg kg}^{-1}$ ), 2-AG levels were elevated by 5-fold at 4 h post-treatment and could be further elevated to 8-10-fold above baseline at higher doses of inhibitor (Fig. 3d). Consistent with previous studies<sup>21</sup>, elevations in brain 2-AG were accompanied by significant reductions in the levels of arachidonic acid (**13**) (Fig. 3e). Other MAGs, such as mono-palmitoylglycerol (**14**) (PG) and mono-oleoylglycerol (**15**) (OG), and their corresponding free fatty acids, palmitic (**16**) and oleic acid (**17**), respectively, were not significantly altered in brains from JZL184-treated animals (Supplementary Fig. 4 online). Importantly, brain anandamide levels were also unaffected by JZL184 at all of the doses tested (Fig. 3f). Other *N*-acyl ethanolamines (NAE), such as *N*-palmitoyl ethanolamine (PEA, **18**), and *N*-oleoyl ethanolamine (OEA, **19**), did not change except at the highest dose of JZL184 tested ( $40 \text{ mg kg}^{-1}$ ), where modest ( $\sim 2$ -fold) elevations in these lipids were observed. The lack of impact of JZL184 on NAE levels is consistent with previous studies showing that partial disruption of FAAH is insufficient to raise NAE levels *in vivo*<sup>33,34</sup>. The lipid profiles of JZL184-treated mice contrasted sharply with those induced by the selective FAAH inhibitor URB597 (**20**), which completely inhibited brain FAAH activity and caused significant elevations in anandamide and other NAEs without altering 2-AG or arachidonic acid levels in this tissue (Fig. 3f and Supplementary Fig. 4 online). Similar data were also obtained following oral administration of JZL184 (Supplementary Fig. 5 online), indicating that this compound can be administered by multiple routes to achieve selective blockade of MAGL *in vivo*.

To determine whether MAGL inhibition also produced increases in signaling-competent release of extracellular 2-AG, we analyzed JZL184-treated mice by *in vivo* microdialysis following neuronal activation<sup>35,36</sup>. JZL184 dramatically elevated the interstitial brain levels of 2-AG following neuronal depolarization (Fig. 4a), but did not affect interstitial brain levels of AEA (Fig. 4b). These data indicate that blockade of MAGL by JZL184 elevates both bulk and signaling-dependent pools of 2-AG in the nervous system.

### Inhibition of MAGL is rapid and persistent in mice

To determine the time course of JZL184 inhibition *in vivo*, mice were administered JZL184 ( $16 \text{ mg kg}^{-1}$ , i.p.) and sacrificed at 0.5, 1, 2, 4, 8, and 24 h for analysis. ABPP of brain membrane proteomes (Fig. 5a) as well as 2-AG and oleamide hydrolysis assays (Fig. 5b) indicated that MAGL inhibition was rapid, with maximal inhibition achieved within 0.5 h post-treatment, and long-lasting, with  $> 80\%$  inhibition of 2-AG hydrolysis activity persisting for at least 24 h (Fig. 5a). In contrast, FAAH blockade occurred much more slowly and never exceeded 70% at any time point examined (Fig. 5b). Concomitant with the rapid inhibition of MAGL, JZL184 treatment caused swift accumulation of 2-AG in the brain. By 0.5 h, brain 2-AG levels were already elevated 7-fold and remained 7-9-fold above control levels for at least 8 h (Fig. 5c). Interestingly, 2-AG levels returned to near-control levels by 24 h, even though  $> 80\%$  of the activity of MAGL remained inhibited at this time point. Elevations in 2-AG were matched by a rapid and sustained decrease in arachidonic acid (Fig. 5d). NAEs, including anandamide, as well as other MAGs and free fatty acids were unchanged throughout the time course analysis of JZL184-treated mice (Fig. 5e and Supplementary Fig. 6 online).

## Behavioral effects of JZL184 in mice

The dramatic and sustained elevations in brain 2-AG levels caused by JZL184 suggested that this inhibitor might induce endocannabinoid-mediated behavioral effects. Direct CB1 agonists are known to promote multiple behavioral effects in rodents, including analgesia, hypomotility, hypothermia, and catalepsy (collectively referred to as the tetrad test for cannabinoid activity<sup>37</sup>). Interestingly, FAAH inhibitors are largely inactive in the tetrad test, causing analgesia, but not other cannabinoid behavioral phenotypes<sup>15</sup>. JZL184 (16 mg kg<sup>-1</sup>, 2 h) was also found to exhibit significant analgesic activity in several pain assays, including the tail-immersion test of acute thermal pain sensation (Fig. 6a), the acetic acid writhing test of visceral pain (Fig. 6b), and the formalin test of noxious chemical pain (Fig. 6c and d). In each case, the effects of JZL184 were blocked by pre-treatment with the CB1 antagonist rimonabant (**21**) (3 mg kg<sup>-1</sup>) (Fig. 6a-d). In marked contrast to FAAH inhibitors, JZL184 also promoted significant hypothermia (Fig. 6e) and hypomotility (Fig. 6f). JZL184 treatment did not, however, induce catalepsy when assessed in the bar test. The hypothermic effect of JZL184 was completely blocked by rimonabant (Fig. 6e), indicating that it is mediated by CB1 receptors. We could not unequivocally determine the contribution of CB1 receptors to the hypomotile effect of JZL184 because rimonabant was found, on its own, to induce significant reductions in movement (as has been previously reported<sup>38</sup>) (Fig. 6f). However, a partial blockade of JZL184-induced immobility was observed with rimonabant (Fig. 6f), suggesting a contribution of CB1 receptors to this phenotype. Finally, JZL184 did not produce significant hypomotility, hypothermia, or analgesia in *CB1*<sup>-/-</sup> mice (Supplementary Fig. 7 online). These data collectively indicate that JZL184 induces a broad array of cannabinoid behavioral effects in rodents that qualitatively mimic much of the pharmacological profile of direct CB1 agonists.

## DISCUSSION

Many neurotransmitter systems exhibit diversification at the level of receptors, where multiple ionotropic and/or metabotropic receptors are activated by a single ligand<sup>39</sup>. The endocannabinoid system is unusual in also possessing at least two physiological ligands, AEA and 2-AG, thus raising provocative questions about the respective roles that these endocannabinoids play in nervous system function. This problem can be experimentally addressed by perturbing the enzymatic pathways responsible for AEA and 2-AG metabolism. For instance, the genetic<sup>13</sup> or pharmacological<sup>14,15</sup> disruption of FAAH has provided evidence that AEA signaling pathways regulate pain, inflammation, and neuropsychiatric processes. Equivalent experimental tools to selectively perturb 2-AG metabolism, however, have been lacking. Here, we have described JZL184, a highly efficacious and selective inhibitor of the 2-AG-degrading enzyme MAGL. That brain 2-AG hydrolysis activity was reduced by ~85% following administration of JZL184 to mice provides *in vivo* confirmation of previous *in vitro* estimates of the principal contribution that MAGL makes to total brain 2-AG hydrolysis activity<sup>20,22</sup>.

Blockade of MAGL activity was sufficient to raise brain 2-AG levels by 8-10 fold. A similar elevation in stimulated release of 2-AG was observed by *in vivo* microdialysis following inhibition of MAGL. Whether further increases in bulk and/or interstitial levels of 2-AG

might occur upon concurrent blockade of additional brain 2-AG hydrolases, such as ABHD6 and ABHD1220, remains unknown. Interestingly, we did not observe changes in baseline interstitial levels of 2-AG following treatment with JZL184 (Fig. 4a), even though this inhibitor was administered to mice 1 h prior to neuronal depolarization (a time period that was sufficient to raise bulk brain 2-AG levels; Fig. 5c). These data could indicate that 2-AG is sequestered intracellularly in neurons prior to depolarization events, which then induce release of this endocannabinoid. The increased brain levels of 2-AG induced by a single dose of JZL184 were maintained for a remarkable period of time (8 h), likely reflecting the relatively long half-life of this inhibitor *in vivo* (~7 h; see Supplementary Fig. 8 online). It is notable, however, that brain 2-AG levels returned to baseline by 24 h post-treatment with JZL184, even though MAGL remained mostly inactive at this time point. These results might indicate a homeostatic feedback mechanism that operates to rectify heightened 2-AG concentrations in the nervous system. JZL184 did not significantly alter the levels of NAEs, including AEA, or other monoacylglycerols, including PG and OG. These data indicate a surprisingly selective role for MAGL in regulating 2-AG in the nervous system. Since MAGL is capable of hydrolyzing other monoacylglycerols *in vitro*, its selective control over 2-AG in the nervous system must reflect other as of yet unknown factors. Possibilities include differences in the mechanisms of biosynthesis of distinct classes of monoacylglycerols and the coupling of these pathways to MAGL, or spatial segregation of MAGL and 2-AG from the other monoacylglycerols.

The rapid and sustained elevations in 2-AG induced by JZL184 were accompanied by a provocative array of CB1-dependent behavioral effects, including analgesia, hypomotility, and hypothermia. This collection of phenotypes qualitatively resembles those induced by direct CB1 agonists<sup>13,37</sup>. However, clear differences were also noted. For instance, JZL184-treated mice did not develop catalepsy and appeared generally normal in terms of their overt posture and appearance (i.e., spontaneous limb splaying was not observed). The hypothermic and analgesic effects caused by JZL184 also appeared lower in magnitude compared to those produced by CB1 agonists<sup>13</sup>. Overall, these data suggest that MAGL-regulated 2-AG pathways endogenously modulate several behavioral processes classically associated with the pharmacology of cannabinoids, which contrasts with the more discrete set of phenotypes observed upon disruption of FAAH. It is perhaps interesting to briefly speculate on the therapeutic implications of these findings. Much of the enthusiasm for FAAH as a potential drug target has stemmed from the lack of overt cannabinoid behavior observed upon disruption of this enzyme<sup>40,41</sup>. One cannot readily arrive at the same conclusion for MAGL, given that blockade of this enzyme produced CB1-dependent phenotypes, such as hypothermia and hypomotility, that might be viewed as undesirable from a medicinal perspective. It remains possible, however, that these phenotypes could be pharmacologically uncoupled from more beneficial effects (e.g., analgesia) by titrating the magnitude of MAGL inhibition *in vivo*. Indeed, we observed significant increases in 2-AG levels across the entire dose-range of JZL184 tested in this study (4–40 mg kg<sup>-1</sup>), even though the lower doses resulted in less blockade of MAGL activity. These data thus indicate that even partial inhibition of MAGL may be sufficient to augment 2-AG-mediated endocannabinoid signaling *in vivo*.

Looking forward, the chemical scaffold of JZL184 should provide a fertile starting point for medicinal chemistry work to improve the properties of MAGL inhibitors. Regarding selectivity, our ABPP studies would argue that, among the more than 40 serine hydrolases expressed in the mammalian brain, the most common “off-target” for MAGL inhibitors will likely be FAAH. Indeed, despite showing greater than 300-fold selectivity for MAGL over FAAH *in vitro*, JZL184 still partially blocked FAAH activity *in vivo*. This partial inhibition, however, did not result in elevated levels of AEA or other NAEs, consistent with previous findings indicating that > 80% blockade of FAAH is required to raise NAEs *in vivo*<sup>34</sup>. Additional serine hydrolase targets of JZL184 may be found in peripheral tissues, such as liver, where carboxylesterases have been shown to be sensitive to carbamate inhibitors<sup>26,42</sup>. Moreover, our functional proteomic screen does not exclude the possibility that JZL184 could interact with other proteins outside of the serine hydrolase class, including enzymes, such as oxidoreductases, that may also participate in 2-AG metabolism<sup>43,44</sup>. Future studies where the behavioral effects of JZL184 are compared to those observed in mice with a genetic deletion of MAGL should further clarify the specificity of JZL184.

In summary, we believe that the properties of JZL184 warrant inclusion of this compound among the growing arsenal of efficacious and selective pharmacological probes to examine the endocannabinoid system<sup>10</sup>. With selective inhibitors now available for two of the principal endocannabinoid degradative enzymes, FAAH and MAGL, investigators are in a position to experimentally discriminate the activities of AEA and 2-AG in a wide range of biological systems. Our initial findings, when integrated with previous studies<sup>14,15</sup>, argue that these endocannabinoids possess distinct, but overlapping functions *in vivo*. The activity displayed by JZL184 in several components of the tetrad test for cannabinoid pharmacology suggests a potentially broad role for MAGL and 2-AG pathways throughout the nervous system. In contrast, FAAH and AEA pathways may participate in a more restricted set of cannabinoid signaling networks *in vivo*. It is finally interesting to consider whether behavioral processes, such as pain sensation, that are regulated by both AEA and 2-AG<sup>6</sup> could be even more strongly affected by dual MAGL-FAAH inhibitors. JZL184 could itself serve as a lead scaffold for the development of such dual inhibitors, given that at high concentrations, this compound inhibited both MAGL and FAAH without significantly affecting other brain serine hydrolases.

## METHODS

### Materials

2-AG, pentadecanoic acid (PDA, **22**), AEA, and URB597 were purchased from Cayman Chemicals (Ann Arbor, MI). Monopentadecanoin (**23**) was purchased from Nu-Chek-Prep, Inc. (Elysian, MN). Tetrahydrolipstatin (THL, **24**) and methyl arachidonoyl fluorophosphonate (MAFP, **25**) was purchased from Sigma (St. Louis, MO). 1-palmitoyl-2-arachidonoyl-*sn*-glycero-3-phosphocholine (PAPC, **26**) and L- $\alpha$ -phosphatidylinositol-4,5-bisphosphate (PIP<sub>2</sub>, **27**) were purchased from Avanti Polar Lipids (Alabaster, AL). L- $\alpha$ -1-palmitoyl-2-arachidonoyl-phosphatidylcholine [arachidonoyl-1-<sup>14</sup>C] (**28**) was purchased from PerkinElmer (Boston, MA). FP-rhodamine (**29**) and FP-biotin were synthesized as described previously<sup>29,45</sup>. Rimbonabant was obtained from NIDA (Rockville, MD) and dissolved in a

vehicle of 18:1:1 v/v/v saline, ethanol, and alkamuls-620 (Rhône-Poulenc, Princeton, NJ).  $^{13}\text{C}$ -oleamide ( $^{13}\text{C}_{18}\text{H}_{35}\text{NO}$ ) was synthesized from  $^{13}\text{C}$ -oleic acid (Spectra Stable Isotopes, Columbia, MD) according to a literature procedure<sup>12</sup>.

### Chemical synthesis of JZL184 (1)

JZL184 was synthesized from 4-bromo-1,2-methylenedioxybenzene (**30**) and ethyl *N*-Cbz-isonipecotate (**31**) in 3 steps and 35% overall yield:  $^1\text{H}$  NMR ( $\text{CDCl}_3$ , 400 MHz)  $\delta$  1.40-1.48 (m, 2H), 1.62-1.69 (m, 2H), 2.16 (s, 1H), 2.48 (t,  $J = 12$  Hz, 1H), 2.88 (t,  $J = 13$  Hz, 1H), 3.1 (t,  $J = 13$  Hz, 1H), 4.30 (t,  $J = 10$  Hz, 2H), 5.93 (s, 4H), 6.75 (d,  $J = 9$  Hz, 2H), 6.91-6.93 (m, 4H), 7.26 (d,  $J = 9$  Hz, 2H), 8.23 (d,  $J = 9$  Hz, 2H);  $^{13}\text{C}$  NMR ( $\text{CDCl}_3$ , 100 MHz)  $\delta$  26.5, 26.9, 44.5, 44.8, 45.2, 79.6, 101.3, 106.9, 108.1, 119.0, 122.5, 125.2, 139.7, 145.0, 146.5, 148.0, 152.3, 156.5; HRMS calculated for  $\text{C}_{27}\text{H}_{24}\text{N}_2\text{NaO}_9$   $[\text{M}+\text{Na}]^+$  543.1374, found 543.1368. See Supplementary Methods online for details on the synthesis of MAGL inhibitors.

### Competitive activity-based protein profiling (ABPP) experiments

*In vitro* inhibitor selectivity was examined using a competitive ABPP method as described previously<sup>30</sup>. Briefly, mouse brain membrane proteomes, prepared as described in the Supplementary Methods online, were diluted to  $1\text{ mg ml}^{-1}$  in PBS and pre-incubated with varying concentrations of inhibitors (1 nM to 10  $\mu\text{M}$ ) for 30 min at  $37^\circ\text{C}$  prior to the addition of a FP-rhodamine at a final concentration of  $2\text{ }\mu\text{M}$  in a  $50\text{ }\mu\text{l}$  of total reaction volume. After 30 min at room temperature, the reactions were quenched with 4X SDS-PAGE loading buffer, boiled for 5 min at  $90^\circ\text{C}$ , subjected to SDS-PAGE, and visualized in-gel using a flatbed fluorescence scanner.

### Enzyme activity assays

MAGL and FAAH substrate hydrolysis assays were performed using previously described liquid chromatography-mass spectrometry (LC-MS) assays<sup>20</sup> as detailed in the Supplementary Methods online.

### *In vitro* studies with JZL184

Standard assays were performed by pre-incubating protein samples with JZL184 for 30 min at  $37^\circ\text{C}$  prior to the addition of substrate or ABPP probe. Concentration-dependence inhibition curves were obtained from substrate assays and were fit using Prism software (GraphPad) to obtain  $\text{EC}_{50}$  values with 95% confidence intervals. For measurement of  $k_{\text{obs}}$   $[\text{I}]^{-1}$  values, brain membrane proteomes ( $1\text{ mg ml}^{-1}$ ,  $300\text{ }\mu\text{l}$  total) were incubated with JZL184 (0.01-15  $\mu\text{M}$ , 10-40 min,  $37^\circ\text{C}$ ). Every 10 min,  $50\text{ }\mu\text{l}$  of the reaction was removed and treated with FP-rhodamine ( $2\text{ }\mu\text{M}$ ) for 2 min, quenched with 4X SDS-PAGE loading buffer, and boiled for 5 min at  $90^\circ\text{C}$ . The combined reactions were subjected to SDS-PAGE and visualized in-gel using a flatbed fluorescence scanner. The percentage activity remaining was determined by measuring the integrated optical density corresponding to the MAGL or FAAH bands and the results were fit to an exponential curve to determine the pseudo-first order rate constants.

### ***In vivo* studies with JZL184**

JZL184 (neat) was dissolved by vortexing, sonicating, and gentle heating directly into 4:1 v/v PEG300:Tween80 (10, 4, 2, or 1 mg ml<sup>-1</sup>). Male C57Bl/6J mice (6-8 weeks old, 20-26 g) were intraperitoneally (i.p.) administered JZL184 or a 4:1 v/v PEG300:Tween80 vehicle without JZL184 at a volume of 4  $\mu$ l g<sup>-1</sup> weight (40, 16, 8, or 4 mg kg<sup>-1</sup> by the dilutions above). After the indicated amount of time, mice were anesthetized with isoflurane and sacrificed by decapitation. Brains were removed, hemisected along the midsagittal plane, and each half was then flash frozen in liquid N<sub>2</sub>. One half of the brain was prepared as described above for protein analysis and the other half was used for metabolite analysis. The selective inhibition of FAAH by URB597 was achieved in a similar manner as described above, except URB597 was dissolved by sonication into 18:1:1 v/v/v saline:emulphor:ethanol (1 mg ml<sup>-1</sup>) and administered i.p. at a volume of 10  $\mu$ l g<sup>-1</sup> weight (10 mg kg<sup>-1</sup> final dose). Oral administration was performed exactly as described for i.p. administration, except that the vehicle was PEG300.

### **Measurement of brain lipids**

Brain lipid measurements were determined using a previously described procedures<sup>33</sup> as detailed in the Supplementary Methods online.

### **ABPP-MudPIT analysis of SH targeted by JZL184 *in vivo***

ABPP-MudPIT studies were performed following previously described methods<sup>27,32</sup> as detailed in the Supplementary Methods online.

### **Behavioral studies**

Mice were evaluated in the tetrad test for cannabinoid effects and the acetic acid-induced stretching assay as detailed in the Supplementary Methods online. Animal experiments were conducted in accordance with guidelines of the Institutional Animal Care and Use Committees of The Scripps Research Institute and Virginia Commonwealth University.

### **Supplementary Material**

Refer to Web version on PubMed Central for supplementary material.

### **Acknowledgments**

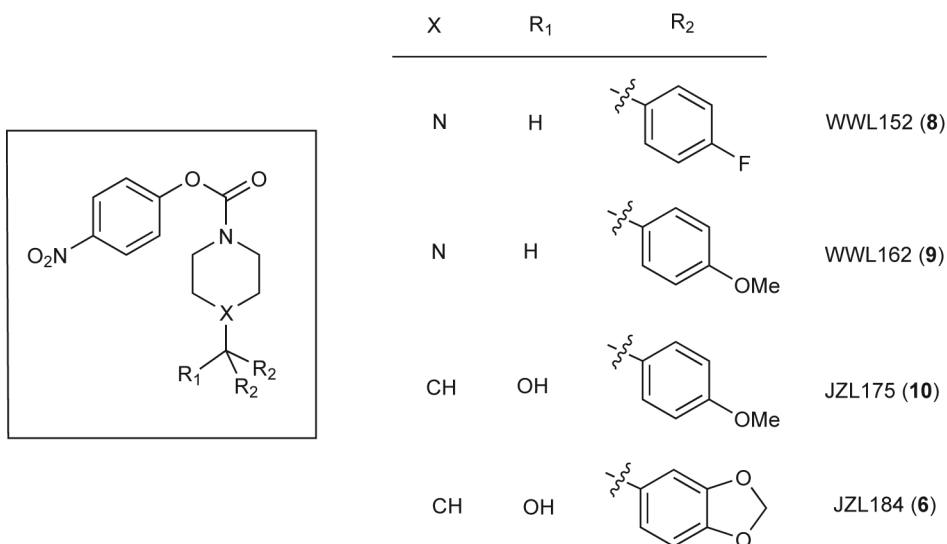
We thank the Cravatt lab for helpful discussion and critical reading of the manuscript. This work was supported by the NIH (DA017259, DA025285, DA007027, DA005274 AA014619, DA024194, AA06420), the Helen L. Dorris Institute Child and Adolescent Neuro-Psychiatric Disorder Institute, and the Skaggs Institute for Chemical Biology.

### **REFERENCES**

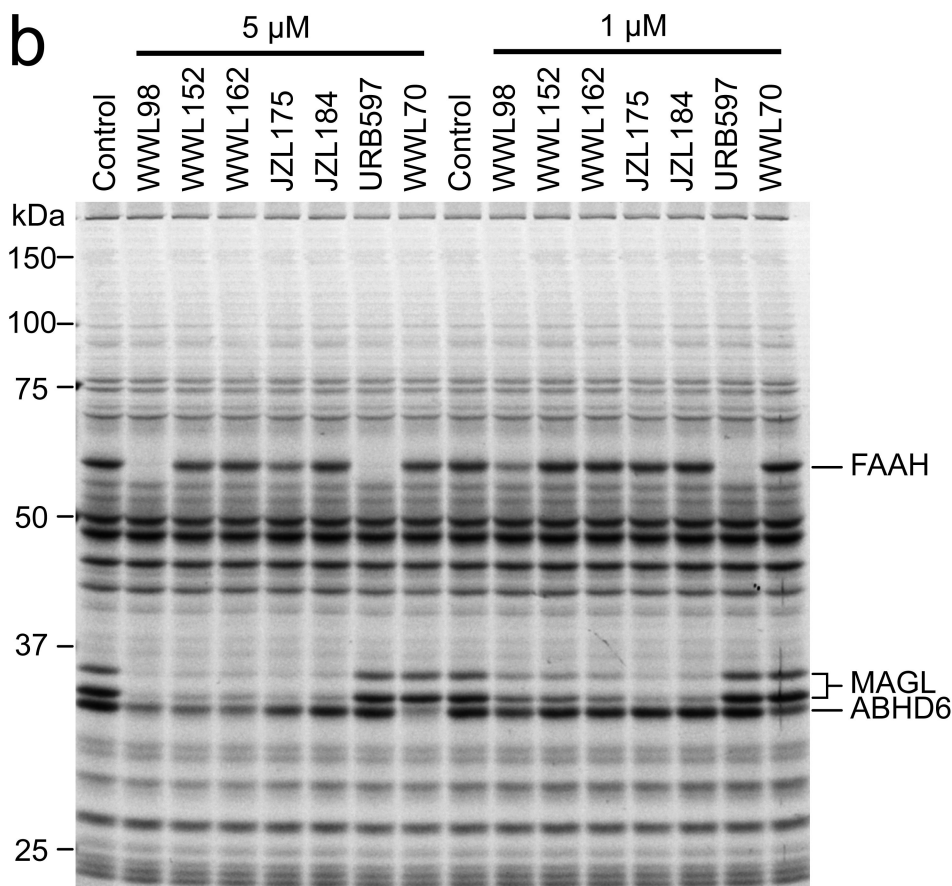
1. Mackie K. Cannabinoid receptors as therapeutic targets. *Annu Rev Pharmacol Toxicol.* 2006; 46:101–22. [PubMed: 16402900]
2. Devane WA, et al. Isolation and structure of a brain constituent that binds to the cannabinoid receptor. *Science.* 1992; 258:1946–9. [PubMed: 1470919]
3. Sugiura T, et al. 2-Arachidonoylglycerol: a possible endogenous cannabinoid receptor ligand in brain. *Biochemical and Biophysical Research Communications.* 1995; 215:89–97. [PubMed: 7575630]

4. Mechoulam R, et al. Identification of an endogenous 2-monoglyceride, present in canine gut, that binds to cannabinoid receptors. *Biochemical Pharmacology*. 1995; 50:83–90. [PubMed: 7605349]
5. Di Marzo V, et al. Leptin-regulated endocannabinoids are involved in maintaining food intake. *Nature*. 2001; 410:822–5. [PubMed: 11298451]
6. Hohmann AG, et al. An endocannabinoid mechanism for stress-induced analgesia. *Nature*. 2005; 435:1108–12. [PubMed: 15973410]
7. Holt S, Comelli F, Costa B, Fowler CJ. Inhibitors of fatty acid amide hydrolase reduce carrageenan-induced hind paw inflammation in pentobarbital-treated mice: comparison with indomethacin and possible involvement of cannabinoid receptors. *Br J Pharmacol*. 2005; 146:467–76. [PubMed: 16100529]
8. Marsicano G, et al. The endogenous cannabinoid system controls extinction of aversive memories. *Nature*. 2002; 418:530–4. [PubMed: 12152079]
9. Varvel SA, Lichtman AH. Evaluation of CB1 receptor knockout mice in the Morris water maze. *J Pharmacol Exp Ther*. 2002; 301:915–24. [PubMed: 12023519]
10. Di Marzo V. Targeting the endocannabinoid system: to enhance or reduce? *Nat Rev Drug Discov*. 2008; 7:438–55. [PubMed: 18446159]
11. Ahn K, McKinney MK, Cravatt BF. Enzymatic pathways that regulate endocannabinoid signaling in the nervous system. *Chemical Reviews*. 2008; 108:1687–707. [PubMed: 18429637]
12. Cravatt BF, et al. Molecular characterization of an enzyme that degrades neuromodulatory fatty-acid amides. *Nature*. 1996; 384:83–87. [PubMed: 8900284]
13. Cravatt BF, et al. Supersensitivity to anandamide and enhanced endogenous cannabinoid signaling in mice lacking fatty acid amide hydrolase. *Proc Natl Acad Sci U S A*. 2001; 98:9371–6. [PubMed: 11470906]
14. Kathuria S, et al. Modulation of anxiety through blockade of anandamide hydrolysis. *Nat Med*. 2003; 9:76–81. [PubMed: 12461523]
15. Lichtman AH, et al. Reversible inhibitors of fatty acid amide hydrolase that promote analgesia: evidence for an unprecedented combination of potency and selectivity. *J Pharmacol Exp Ther*. 2004; 311:441–8. [PubMed: 15229230]
16. Ahn K, McKinney MK, Cravatt BF. Enzymatic pathways that regulate endocannabinoid signaling in the nervous system. *Chem Rev*. 2008; 108:1687–707. [PubMed: 18429637]
17. Cravatt BF, et al. Supersensitivity to anandamide and enhanced endogenous cannabinoid signaling in mice lacking fatty acid amide hydrolase. *Proc. Natl. Acad. Sci. U.S.A.* 2001; 98:9371–9376. [PubMed: 11470906]
18. Dinh TP, et al. Brain monoglyceride lipase participating in endocannabinoid inactivation. *Proceedings of the National Academy of Sciences of the United States of America*. 2002; 99:10819–24. [PubMed: 12136125]
19. Dinh TP, Kathuria S, Piomelli D. RNA interference suggests a primary role for monoacylglycerol lipase in the degradation of the endocannabinoid 2-arachidonoylglycerol. *Molecular Pharmacology*. 2004; 66:1260–4. [PubMed: 15272052]
20. Blankman JL, Simon GM, Cravatt BF. A Comprehensive Profile of Brain Enzymes that Hydrolyze the Endocannabinoid 2-Arachidonoylglycerol. *Chem Biol*. 2007; 14:1347–56. [PubMed: 18096503]
21. Nomura DK, et al. Activation of the endocannabinoid system by organophosphorus nerve agents. *Nat Chem Biol*. 2008; 4:373–8. [PubMed: 18438404]
22. Saario SM, et al. Characterization of the sulfhydryl-sensitive site in the enzyme responsible for hydrolysis of 2-arachidonoyl-glycerol in rat cerebellar membranes. *Chem Biol*. 2005; 12:649–56. [PubMed: 15975510]
23. King AR, et al. URB602 inhibits monoacylglycerol lipase and selectively blocks 2-arachidonoylglycerol degradation in intact brain slices. *Chem Biol*. 2007; 14:1357–65. [PubMed: 18096504]
24. Vandevoorde S, et al. Lack of selectivity of URB602 for 2-oleoylglycerol compared to anandamide hydrolysis in vitro. *Br J Pharmacol*. 2006

25. Burston JJ, et al. N-Arachidonyl maleimide (NAM) potentiates the pharmacological and biochemical effects of the endocannabinoid 2-arachidonylglycerol through inhibition of monoacylglycerol lipase. *J Pharmacol Exp Ther.* 2008
26. Alexander JP, Cravatt BF. Mechanism of carbamate inactivation of FAAH: implications for the design of covalent inhibitors and in vivo functional probes for enzymes. *Chem Biol.* 2005; 12:1179–87. [PubMed: 16298297]
27. Li W, Blankman JL, Cravatt BF. A Functional Proteomic Strategy to Discover Inhibitors for Uncharacterized Hydrolases. *J. Am. Chem. Soc.* 2007; 129:9594–9595. [PubMed: 17629278]
28. Cravatt BF, Wright AT, Kozarich JW. Activity-based protein profiling: from enzyme chemistry to proteomic chemistry. *Annu Rev Biochem.* 2008; 77:383–414. [PubMed: 18366325]
29. Liu Y, Patricelli MP, Cravatt BF. Activity-based protein profiling: the serine hydrolases. *Proc Natl Acad Sci U S A.* 1999; 96:14694–9. [PubMed: 10611275]
30. Leung D, Hardouin C, Boger DL, Cravatt BF. Discovering potent and selective inhibitors of enzymes in complex proteomes. *Nat. Biotechnol.* 2003; 21:687–691. [PubMed: 12740587]
31. Greenbaum D, et al. Chemical approaches for functionally probing the proteome. *Mol. Cell. Proteomics.* 2002; 1:60–68. [PubMed: 12096141]
32. Jessani N, et al. A streamlined platform for high-content functional proteomics of primary human specimens. *Nat Methods.* 2005; 2:691–7. [PubMed: 16118640]
33. Cravatt BF, et al. Functional disassociation of the central and peripheral fatty acid amide signaling systems. *Proc Natl Acad Sci U S A.* 2004; 101:10821–6. [PubMed: 15247426]
34. Fegley D, et al. Characterization of the fatty acid amide hydrolase inhibitor cyclohexyl carbamic acid 3'-carbamoyl-biphenyl-3-yl ester (URB597): effects on anandamide and oleylethanolamide deactivation. *Journal of Pharmacology and Experimental Therapeutics.* 2005; 313:352–8. [PubMed: 15579492]
35. Caille S, Alvarez-Jaimes L, Polis I, Stouffer DG, Parsons LH. Specific Alterations of Extracellular Endocannabinoid Levels in the Nucleus Accumbens by Ethanol, Heroin, and Cocaine Self-Administration. *J. Neurosci.* 2007; 27:3695–3702. [PubMed: 17409233]
36. Bequet F, et al. CB1 receptor-mediated control of the release of endocannabinoids (as assessed by microdialysis coupled with LC/MS) in the rat hypothalamus. *Eur J Neurosci.* 2007; 26:3458–3464. [PubMed: 18052990]
37. Wiley JL, Martin BR. Cannabinoid pharmacological properties common to other centrally acting drugs. *Eur J Pharmacol.* 2003; 471:185–93. [PubMed: 12826237]
38. Compton DR, Aceto MD, Lowe J, Martin BR. In vivo characterization of a specific cannabinoid receptor antagonist (SR141716A): inhibition of delta 9-tetrahydrocannabinol-induced responses and apparent agonist activity. *J Pharmacol Exp Ther.* 1996; 277:586–94. [PubMed: 8627535]
39. Siegel, GJ.; Agranoff, BW.; Albers, RW.; Molinoff, PB. *Basic Neurochemistry.* Raven Press; New York: 1994. p. 182-183.
40. Piomelli D, et al. Pharmacological profile of the selective FAAH inhibitor KDS-4103 (URB597). *CNS Drug Rev.* 2006; 12:21–38. [PubMed: 16834756]
41. Cravatt BF, Lichtman AH. Fatty acid amide hydrolase: an emerging therapeutic target in the endocannabinoid system. *Curr. Opin. Chem. Biol.* 2003; 7:469–475. [PubMed: 12941421]
42. Zhang D, et al. Fatty acid amide hydrolase inhibitors display broad selectivity and inhibit multiple carboxylesterases as off-targets. *Neuropharmacology.* 2007; 52:1095–105. [PubMed: 17217969]
43. Chen JK, et al. Identification of novel endogenous cytochrome p450 arachidonate metabolites with high affinity for cannabinoid receptors. *J Biol Chem.* 2008; 283:24514–24. [PubMed: 18606824]
44. Kozak KR, Rowlinson SW, Marnett LJ. Oxygenation of the endocannabinoid, 2-arachidonylglycerol, to glyceryl prostaglandins by cyclooxygenase-2. *J Biol Chem.* 2000; 275:33744–9. [PubMed: 10931854]
45. Patricelli MP, Giang DK, Stamp LM, Burbaum JJ. Direct visualization of serine hydrolase activities in complex proteomes using fluorescent active site-directed probes. *Proteomics.* 2001; 1:1067–71. [PubMed: 11990500]
46. Karlsson M, et al. Exon-intron organization and chromosomal localization of the mouse monoglyceride lipase gene. *Gene.* 2001; 272:11–18. [PubMed: 11470505]

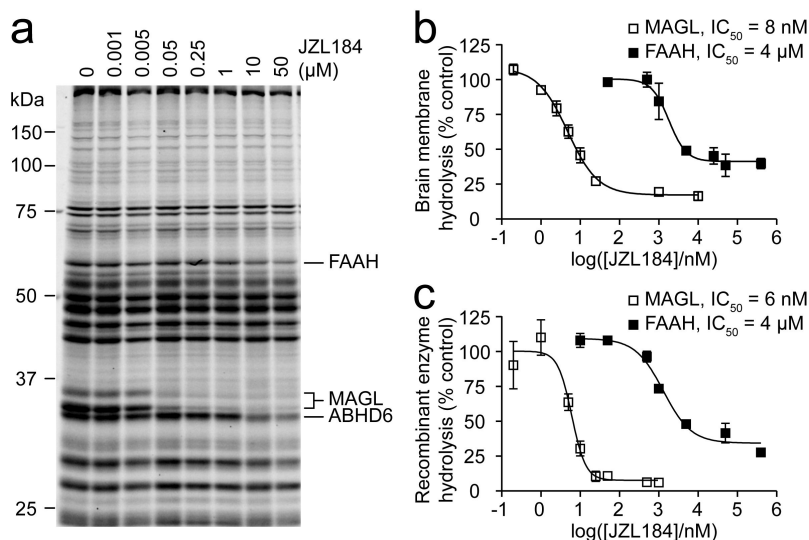


**Fig. 1.** Structures and competitive ABPP profiles of MAGL inhibitors. **a**, Structures of MAGL inhibitors. **b**, Competitive ABPP showing the effect of MAGL inhibitors on serine hydrolase activities in the mouse brain membrane proteome. Shown for comparison are the profiles of the selective FAAH and ABHD6 inhibitors, URB59714 and WWL70 (**32**)<sup>27</sup> respectively. Inhibitors were incubated with brain membranes for 30 min, followed by treatment with the serine hydrolase-directed ABPP probe FP-rhodamine (2  $\mu$ M, 30 min), and the proteomes were then analyzed by SDS-PAGE and in-gel fluorescence scanning to detect inhibited enzymes. Control proteomes were treated with DMSO alone. Fluorescent gel is shown in grayscale. Note that brain MAGL migrates as a 35 kDa doublet by SDS-PAGE, as reported previously<sup>20,46</sup>.



**Fig. 2.**

*In vitro* characterization of JZL184. **a**, Concentration-dependent effects of JZL184 on mouse brain membrane serine hydrolases as determined by competitive ABPP. **b**, Blockade of brain membrane MAGL and FAAH activity by JZL184 as determined with substrate assays (2-AG and oleamide, respectively). **c**, Blockade of recombinant MAGL and FAAH activity by JZL184 as determined with substrate assays (2-AG and anandamide, respectively). Enzymes were recombinantly expressed in COS7 cells. Note that JZL184 produced a near-complete blockade of recombinant MAGL activity (> 95%), but ~15% residual 2-AG hydrolysis activity was observed in brain membranes, likely reflecting the activity of other enzymes<sup>20</sup>. For **a-c**, samples were treated with JZL184 for 30 min prior to analysis. For **b** and **c**, data are presented as means  $\pm$  SEM for three independent experiments.

**Fig. 3.**

*In vivo* characterization of JZL184. **a** and **b**, Serine hydrolase activity profiles (**a**) and MAGL and FAAH activities (**b**) of brain membranes prepared from mice treated with JZL184 at the indicated doses (4–40 mg kg<sup>-1</sup>, i.p.) for 4 h. **c**, ABPP-MudPIT analysis of serine hydrolase activities in brain membranes prepared from mice treated with JZL184 (16 mg kg<sup>-1</sup>, i.p., 4 h). MAGL and FAAH control signals are shown in red and blue bars, respectively. **d-f**, Brain levels of 2-AG (**d**), arachidonic acid (**e**), and NAEs (**f**) from mice treated with JZL184 at the indicated doses (4–40 mg kg<sup>-1</sup>, i.p.) for 4 h. For **f**, data from mice treated with URB597 (10 mg kg<sup>-1</sup>, i.p.) are also shown, confirming the elevations of NAEs induced by this FAAH inhibitor. For **b-f**, \*,  $p < 0.05$ ; \*\*,  $p < 0.01$  for inhibitor-treated versus vehicle-treated animals. Data are presented as means  $\pm$  SEM.  $n = 3-5$  mice per group.

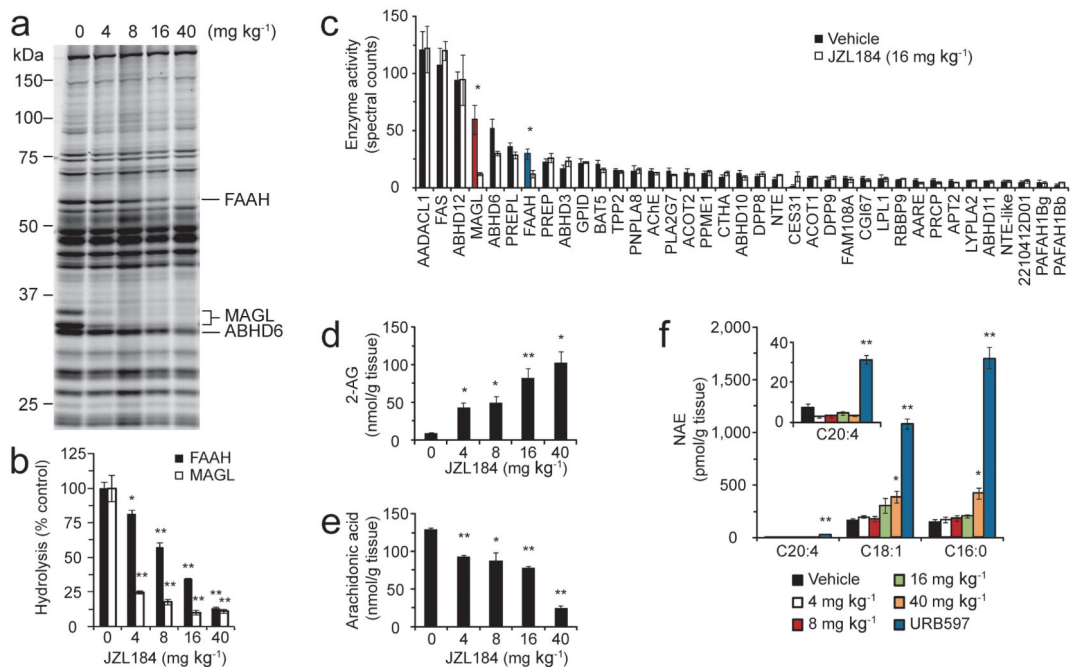


**Fig. 4.**

JZL184 raises interstitial levels of 2-AG following neuronal depolarization. Effects of JZL184 (10 mg kg<sup>-1</sup>, i.p.) on interstitial levels of 2-AG and AEA were measured by *in vivo* microdialysis sampling from the nucleus accumbens of C57Bl/6 mice. Endocannabinoid release was stimulated by neuronal depolarization during perfusion with a high potassium & calcium artificial CSF solution (t = 0-90 min; shaded bar). Depolarization significantly increased dialysate 2-AG levels in both vehicle-(F(10,50) = 2.12, *p* < 0.05) and JZL184-treated (F(10,70) = 5.567, *p* < 0.0001) mice and this effect was substantially more robust in JZL184 treated animals as demonstrated by analysis of both the temporal profile (pretreatment x time interaction (F(10,120) = 3.355, \*, *p* < 0.001; **a**) and area under the curve (AUC) measures (AUC *t* = 0-150 min; F(1,12) = 8.737; \*, *p* < 0.05; **b**). There was no significant alteration in dialysate AEA levels following JZL184 administration and no significant effect of the high potassium/calcium solution on dialysate AEA levels in either group of mice as determined by analysis of both temporal profile and AUC measures (**c** and **d**). Data are the mean ± SEM of the percent change from baseline levels. Baseline dialysate 2-AG levels were 4.6 ± 0.7 nM and 4.2 ± 0.4 nM and dialysate AEA levels were 0.54 ± 0.1 nM vs. 0.58 ± 0.08 nM for the JZL184 (*n* = 8) and vehicle (*n* = 6) groups, respectively. Pretreatments with JZL184 were administered at t = -60 min (denoted by arrow).

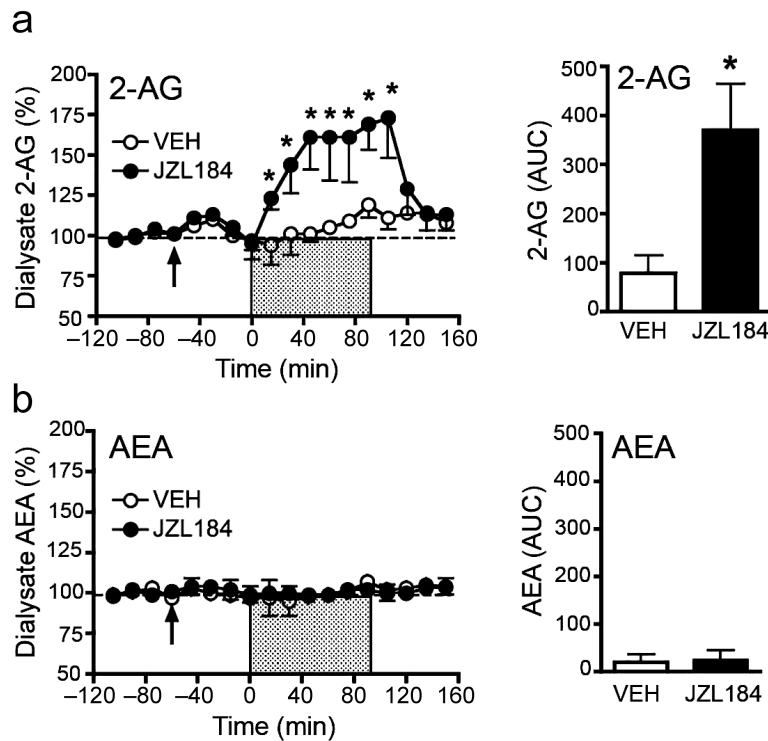


**Fig. 5.** Time course analysis of inhibitory activity of JZL184 *in vivo*. **a** and **b**, Serine hydrolase activity profiles (**a**) and MAGL and FAAH activities (**b**) of brain membranes prepared from mice treated with JZL184 (16 mg kg<sup>-1</sup>, i.p.) for the indicated times. **c-e**, Brain levels of 2-AG (**c**), arachidonic acid (**d**), and AEA (**e**) from mice treated with JZL184 (16 mg kg<sup>-1</sup>, i.p.) for the indicated times. For **b-e**, \*,  $p < 0.05$ ; \*\*,  $p < 0.01$  for inhibitor-treated versus vehicle-treated control animals. Data are presented as means  $\pm$  SEM.  $n = 3-5$  mice per group.

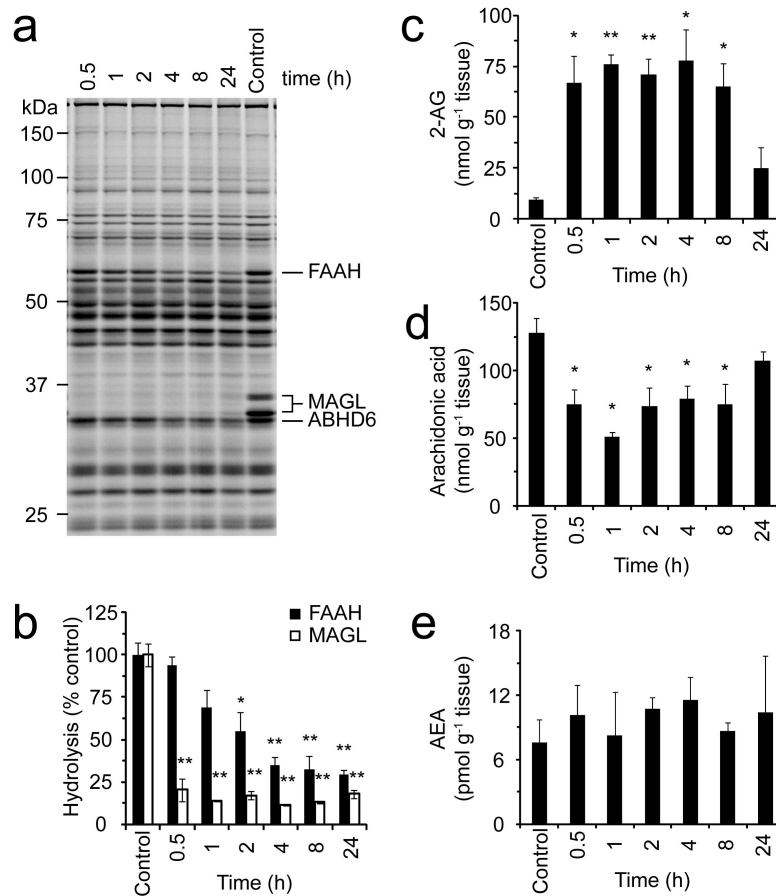


**Fig. 6.** Behavioral effects of JZL184. **a-d**, JZL184 produced antinociceptive effects in the tail immersion assay of thermal pain sensation (**a**; 16 mg kg<sup>-1</sup>, i.p.), acetic acid abdominal stretching assay of noxious chemical pain sensation (**b**; 16 mg kg<sup>-1</sup>, i.p.), and both phase 1 (**c**; 40 mg kg<sup>-1</sup>, p.o.) and phase 2 (**d**; 40 mg kg<sup>-1</sup>, p.o.) of the formalin test. These effects were blocked by pre-treatment with the CB1 antagonist rimonabant (Rim., 3 mg kg<sup>-1</sup>). JZL184 (16 mg kg<sup>-1</sup> i.p.) also produced significant hypothermia (**e**) and hypomotility (**f**) that were significantly attenuated by rimonabant. The baseline tail immersion latency and rectal temperature was 0.82 ± 0.02 s and 37.4 ± 0.1°C, respectively. \*, *p* < 0.05; \*\*, *p* < 0.01, for vehicle-vehicle versus vehicle-JZL184-treated mice. #, *p* < 0.05; ##, *p* < 0.01, for vehicle-JZL184 versus rimonabant-JZL184-treated mice. Data are presented as means ± SEM. *n* = 6-14 mice per group.

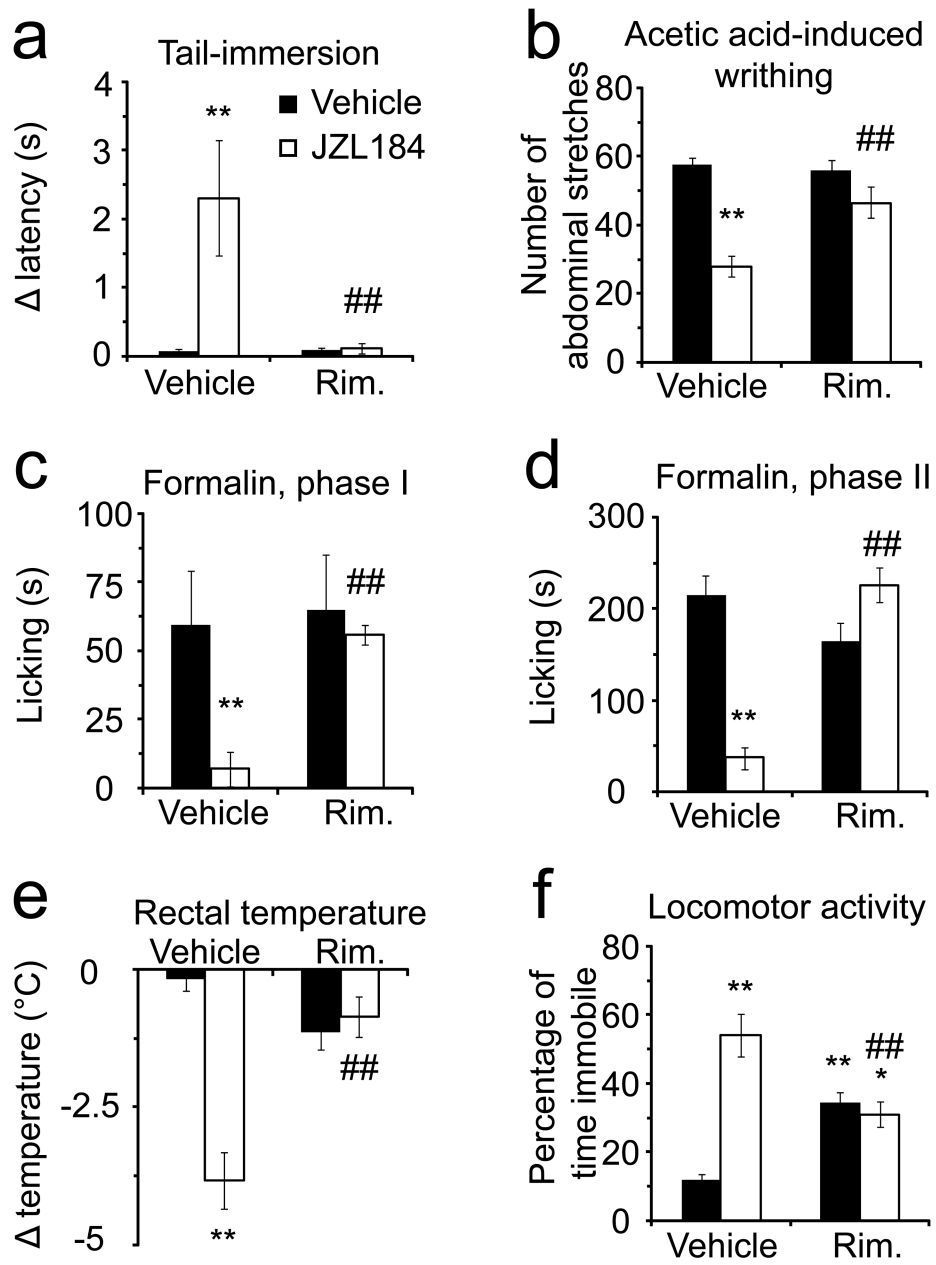


Fig. 7.

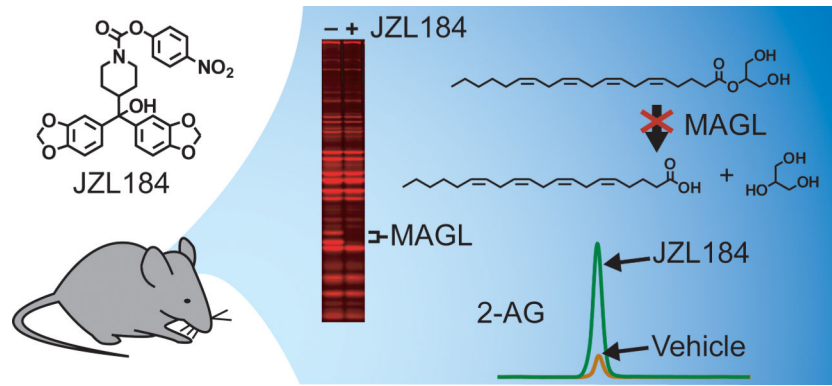


Fig. 8.